Quantum simulation with natural decoherence

C. H. Tseng,[1] S. Somaroo,[1] Y. Sharf,[1] E. Knill,[2] R. Laflamme,[2] T. F. Havel,[3] and D. G. Cory[1,*]
[1]*Department of Nuclear Engineering, Massachusetts Institute of Technology, Cambridge, Massachusetts 02139*
[2]*Theoretical Physics Division, Los Alamos National Laboratory, Los Alamos, New Mexico 87455*
[3]*BCMP Harvard Medical School, 240 Longwood Avenue, Boston, Massachusetts 02115*
(Received 28 February 2000; published 17 August 2000)

A quantum system may be efficiently simulated by a quantum information processor as suggested by Feynman and developed by Lloyd, Wiesner, and Zalka. Within the limits of the experimental implementation, simulation permits the design and control of the kinematic and dynamic parameters of a quantum system. Extension to the inclusion of the effects of decoherence, if approached from a full quantum-mechanical treatment of the system and the environment, or from a semiclassical fluctuating field treatment (Langevin), requires the difficult access to dynamics on the time scale of the environment correlation time. Alternatively, a quantum-statistical approach may be taken which exploits the natural decoherence of the experimental system, and requires a more modest control of the dynamics. This is illustrated for quantum simulations of a four-level quantum system by a two-spin NMR ensemble quantum information processor.

PACS number(s): 03.67.−a, 76.60.−k

I. INTRODUCTION

In the study of quantum systems, the effect of coupling to an environment is inevitably encountered. The desire is often to minimize this effect in order to address only the quantum system, but sometimes one wishes to consider the entire system including the environment. Control of the environment has been achieved [1], notably in quantum optics experiments, through modifying the mode density or symmetry of the reservoir either through temperature or cavity manipulations. Recently, engineered reservoirs have been constructed for quantum computational systems [2,3]. Decoherence due to the environment places limits on the length and complexity of quantum simulations and computation [4–7]. To some extent this can be avoided using methods of quantum error correction [8–16]. These methods require ancillary degrees of freedom upon which are deposited some of the entropy arising from environmental interactions, thereby allowing the encoded degrees of freedom to be protected from decoherence. A complementary strategy is to shape a desired decoherence behavior from the natural decoherence through appropriate control [17,18]. One can, in principle, control decoherence in open systems using operations $U=U(t)$ that are fast compared to the correlation time of the bath $\Delta t \sim \tau_c$ [19–21]. This time scale can, however, be prohibitively short in most accessible cases. In addition, the effect of the control operations will alter the original Hamiltonian and must be accounted for. A treatment of coupling to a coherent external field is given in [22].

The goal of this paper is to examine the unavoidable decoherence effects when a quantum information processor is used to simulate another quantum system. There are two related questions: (i) how is decoherence manifested in a quantum simulation, and (ii) how can decoherence effects as they appear in the simulated system be manipulated? Ignoring decoherence, an explicit simulation [23] of one quantum system by another, namely the simulation of the kinematics and dynamics of a truncated undriven harmonic oscillator and a driven anharmonic oscillator, has been demonstrated by an NMR quantum information processor. This paper aims to extend that simulation method to include decoherence effects, and to illustrate the principles with a simple NMR ensemble quantum system. It is suggested here that some degree of control of decoherence may be achieved in a simulated system by varying the choice of mapping between the physical and simulated systems. Similar approaches have been utilized in NMR [24,25]. The natural decoherence behavior is tied to the physical system, but is manifested in different ways in the simulated system depending on the particular mapping. In the absence of natural decoherence, there are many equivalent mappings that will create a particular simulation. If several appropriate mappings, exploiting special decoherence symmetries, were implemented in series, one may design the overall effective decoherence appearing in the simulated system. Decoherence cannot be eliminated with this method, and the available signal will decay exponentially with the length of the simulation, but the effective decoherence as a deviation against a decaying background may be controlled, allowing the simulation to remain faithful up to a scaling factor. These series are motivated in part by what is possible using refocusing techniques in nuclear magnetic resonance. In the average Hamiltonian sense, these series are analogous to modifying the environmental cavity mode structure.

II. QUANTUM SIMULATION WITHOUT RELAXATION

Using a classical device, the simulation of a quantum system in general is a difficult problem requiring time or memory resources that scale exponentially with the size of the system. However, this is not the case for a universal quantum simulator [26] which uses one quantum system to simulate another quantum system. In particular, it has been shown that an arbitrary local Hamiltonian may be efficiently

*Electronic address: dcory@mit.edu

approximated using a sparsely coupled array of two-state systems [27–30].

To simulate the evolution of a quantum system S under a propagator U, $|s\rangle \xrightarrow{U} |s(T)\rangle$, using a physical system P (a quantum computer) and available operations, S is related to P by an invertible map ϕ which determines a correspondence between all the operators and states of S and of P. The propagator U maps to $V_T = \phi U \phi^{-1}$, and must be implemented using the available external interactions V_i with intervening periods of natural evolution $e^{-i\mathcal{H}_P^0 t/\hbar}$ in P so that $V_T = \Pi_i e^{-i\mathcal{H}_P^0 t_i(T)} V_i$. Any operator (in particular V_T) can be composed of natural evolutions in P and external interactions if a sufficient class of simple operations (logic gates) are implementable in the physical system [31,32]. This general scheme for quantum simulation is represented by the commutative diagram (where the simulated time flows from top to bottom):

$$\begin{array}{ccc} \textbf{Simulated(S)} & & \textbf{Physical(P)} \\ |s\rangle & \xrightarrow{\phi} & |p\rangle \\ {\scriptstyle U=e^{-i\mathcal{H}_S T/\hbar}}\downarrow & & \downarrow{\scriptstyle V_T} \\ |s(T)\rangle & \xleftarrow{\phi^{-1}} & |p_T\rangle. \end{array} \tag{2.1}$$

For unitary maps ϕ, we may write $V_T = e^{-i\bar{\mathcal{H}}_P T/\hbar}$, where $\bar{\mathcal{H}}_P \equiv \phi \bar{\mathcal{H}}_S \phi^\dagger$ can be identified with the average Hamiltonian of Waugh [33]. Many of the concepts of quantum simulation are implicit in the average Hamiltonian theory used to design NMR pulse sequences which implement a specific desired effective Hamiltonian. After the computation in the physical system $|p\rangle \xrightarrow{V_T} |p_T\rangle$, the map ϕ^{-1} identifies $|p_T\rangle \to |s(T)\rangle$ thereby completing the simulation $|s\rangle \to |s(T)\rangle$. Note that the physical times $t_i(T)$ are parametrized by the simulated time T. Also, the dimension of the Hilbert space of the quantum computer must be at least as large as that of the simulated system. In the case of an NMR quantum computer [34,35], for example, the kinematics of any 2^N level quantum system may be simulated using a given N-spin $\frac{1}{2}$ molecule. In what follows, the simulation procedure is illustrated with a (four-level) two-spin molecule. There are advantages and drawbacks to an ensemble NMR quantum computer; nevertheless, the scheme introduced here should be applicable to any realization of a quantum computer. The NMR implementation permits an initial investigation of the principles of quantum computation and simulation.

A. Basis mappings

The simulated quantum system is associated with the physical quantum computer through a basis mapping, which also dictates the associated operators in the two systems. For the two-spin, four-level system the Hamiltonian can be written as

$$\mathcal{H}_S = \mathcal{E}_0|\psi_0\rangle\langle\psi_0| + \mathcal{E}_1|\psi_1\rangle\langle\psi_1| + \mathcal{E}_2|\psi_2\rangle\langle\psi_2| + \mathcal{E}_3|\psi_3\rangle\langle\psi_3|, \tag{2.2}$$

where the $\mathcal{E}_j$ are energy eigenvalues (in no particular order) and $|\psi_j\rangle$ are the corresponding energy eigenstates. Under the mapping to a two-spin system $|\psi_k\rangle \xrightarrow{\phi} |$ binary expansion of $k\rangle$:

$$\begin{aligned} |\psi_0\rangle &\xrightarrow{\phi} |\uparrow\uparrow\rangle, \\ |\psi_1\rangle &\xrightarrow{\phi} |\uparrow\downarrow\rangle, \\ |\psi_2\rangle &\xrightarrow{\phi} |\downarrow\uparrow\rangle, \\ |\psi_3\rangle &\xrightarrow{\phi} |\downarrow\downarrow\rangle. \end{aligned} \tag{2.3}$$

$\mathcal{H}_s$ maps to

$$\begin{aligned} \tilde{\mathcal{H}}_P = \sum_{k=0}^{3} \mathcal{E}_k E_k &= \mathcal{E}_0|\uparrow\uparrow\rangle\langle\uparrow\uparrow| + \mathcal{E}_1|\uparrow\downarrow\rangle\langle\uparrow\downarrow| \\ &+ \mathcal{E}_2|\downarrow\uparrow\rangle\langle\downarrow\uparrow| + \mathcal{E}_3|\downarrow\downarrow\rangle\langle\downarrow\downarrow|, \end{aligned} \tag{2.4}$$

which may also be written, where η_j^k is the jth bit of k,

$$\begin{aligned} \bar{\mathcal{H}}_P &= \sum_{k=0}^{3} \alpha_k (\sigma_z^1)^{\eta_1^k} (\sigma_z^2)^{\eta_2^k}, \\ &= \alpha_0 + \alpha_1 \sigma_z^1 + \alpha_2 \sigma_z^2 + \alpha_3 \sigma_z^1 \sigma_z^2, \end{aligned} \tag{2.5}$$

where it follows from the definition of the Pauli matrices that [36]

$$\begin{aligned} \alpha_0 &= \frac{1}{4}(\mathcal{E}_0 + \mathcal{E}_1 + \mathcal{E}_2 + \mathcal{E}_3), \\ \alpha_1 &= \frac{1}{4}(\mathcal{E}_0 - \mathcal{E}_1 + \mathcal{E}_2 - \mathcal{E}_3), \\ \alpha_2 &= \frac{1}{4}(\mathcal{E}_0 + \mathcal{E}_1 - \mathcal{E}_2 - \mathcal{E}_3), \\ \alpha_3 &= \frac{1}{4}(\mathcal{E}_0 - \mathcal{E}_1 - \mathcal{E}_2 + \mathcal{E}_3). \end{aligned} \tag{2.6}$$

In general, the vector $\boldsymbol{\alpha}$ may be expressed in terms of the energies $\boldsymbol{\mathcal{E}}$:

$$\boldsymbol{\alpha} = 2^{-n} \mathbf{M}^T \boldsymbol{\mathcal{E}}. \tag{2.7}$$

The matrix $\mathbf{M}^T$ is called the Hadamard $2^n \times 2^n$ matrix [37].

B. Truncated quantum harmonic oscillator

The above procedure may be applied to the simulation of a truncated quantum harmonic oscillator (TQHO). This is shown for two different mappings, ϕ_0 and ϕ_1, introduced

here, for which the simulation exhibits markedly different relaxation behavior; however, without decoherence, the mappings are equivalent.

The Hamiltonian for a harmonic oscillator truncated to the first four energy eigenstates, $|n\rangle$, is

$$\mathcal{H}_S=\hbar\Omega/2(|0\rangle\langle 0|+3|1\rangle\langle 1|+5|2\rangle\langle 2|+7|3\rangle\langle 3|). \tag{2.8}$$

Consider the map ϕ_0 for the simulation of the truncated harmonic oscillator,

$$\begin{aligned}
&|n=0\rangle \overset{\phi_0}{\rightarrow} |\uparrow\uparrow\rangle \equiv |a\rangle,\\
&|n=1\rangle \overset{\phi_0}{\rightarrow} |\uparrow\downarrow\rangle \equiv |b\rangle,\\
&|n=3\rangle \overset{\phi_0}{\rightarrow} |\downarrow\uparrow\rangle \equiv |c\rangle,\\
&|n=2\rangle \overset{\phi_0}{\rightarrow} |\downarrow\downarrow\rangle \equiv |d\rangle.
\end{aligned} \tag{2.9}$$

This maps the Hamiltonian to

$$\begin{aligned}
\overline{\mathcal{H}}_P&=\sum_{k=0}^{3}\mathcal{E}_k E_k\\
&=\hbar\Omega/2(|a\rangle\langle a|+3|b\rangle\langle b|+5|d\rangle\langle d|+7|c\rangle\langle c|),
\end{aligned} \tag{2.10}$$

which implies

$$\begin{aligned}
&\mathcal{E}_0=\frac{1}{2}\hbar\Omega,\\
&\mathcal{E}_1=\frac{3}{2}\hbar\Omega,\\
&\mathcal{E}_2=\frac{7}{2}\hbar\Omega,\\
&\mathcal{E}_3=\frac{5}{2}\hbar\Omega,
\end{aligned} \Rightarrow \begin{cases}
\alpha_0=2\hbar\Omega,\\
\alpha_1=0,\\
\alpha_2=-\hbar\Omega,\\
\alpha_3=-\dfrac{1}{2}\hbar\Omega.
\end{cases} \tag{2.11}$$

Equation (2.5) then becomes $\overline{\mathcal{H}}_P^0=\hbar\Omega(2-\sigma_z^2-\frac{1}{2}\sigma_z^1\sigma_z^2)$. Given the internal Hamiltonian for the weakly coupled liquid state NMR two-spin system (in the rotating frame ω_0),

$$\mathcal{H}_0=\left(\frac{\hbar}{2}\right)[(\omega_1-\omega_0)\sigma_z^1+(\omega_2-\omega_0)\sigma_z^2+\pi J\sigma_z^1\sigma_z^2], \tag{2.12}$$

$\overline{\mathcal{H}}_P$ is implemented by the pulse sequence

$$V_T^0=\left(\frac{\tau_1^0}{2}-\pi_y^{12}-\frac{\tau_1^0}{2}+\pi_y^{12}+\tau_2^0\right) \tag{2.13}$$

with $\omega_0=\omega_1$ and delays

$$\tau_1^0=-\Omega T\left(\frac{1}{\pi J}-\frac{2}{(\omega_2-\omega_1)}\right), \tag{2.14}$$

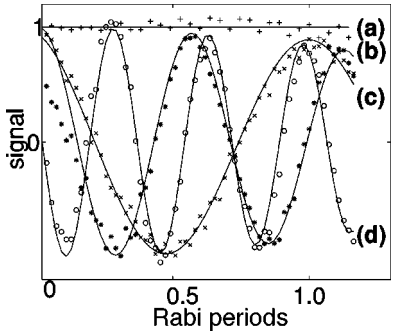

FIG. 1. NMR peak signals from 2,3-dibromothiophene demonstrating a quantum simulation of a truncated harmonic oscillator as implemented by the mapping ϕ_0. Various initial states will express oscillations according to the energy differences between the eigenstates involved. Evolution of the initial states expresses oscillations according to the energy differences between the eigenstates involved: (a) $|0\rangle$ (0Ω), (b) $|0\rangle+i|2\rangle$ (2Ω), and $|0\rangle+|1\rangle+|2\rangle+|3\rangle$ [(c) Ω and (d) 3Ω shown]. The solid lines are to guide the eye.

$$\tau_2^0=-2\Omega T\left(\frac{1}{(\omega_2-\omega_1)}\right).$$

Here π_y^{12}, for example, refers to a radio-frequency pulse on spins 1 and 2 with a rotation of angle π about the y axis. Note that π^{12} is just $(ad)(bc)$, the two cycle permutations $a\leftrightarrow d$ and $b\leftrightarrow c$, and that it is possible to simulate negative times T for the unitary dynamics. The negative signs in $\tau_{1,2}^0$ may be accommodated by considering the refocused phases modulo 2π. For short simulation times, the expected sinusoidal behavior of the populations of the harmonic oscillator is verified for several different initial states (see Fig. 1).

Similarly, the map, ϕ_1, can be defined where up is switched with down for spin 2:

$$\begin{aligned}
&|n=1\rangle \overset{\phi_1}{\rightarrow} |\uparrow\uparrow\rangle = |a\rangle,\\
&|n=0\rangle \overset{\phi_1}{\rightarrow} |\uparrow\downarrow\rangle = |b\rangle,\\
&|n=2\rangle \overset{\phi_1}{\rightarrow} |\downarrow\uparrow\rangle = |c\rangle,\\
&|n=3\rangle \overset{\phi_1}{\rightarrow} |\downarrow\downarrow\rangle = |d\rangle.
\end{aligned} \tag{2.15}$$

This gives $\overline{\mathcal{H}}_P^1=\hbar\Omega(2+\sigma_z^2+1/2\sigma_z^1\sigma_z^2)$, and the pulse sequence

$$V_T^1=\left(\pi_y^2-\frac{\tau_1^1}{2}-\pi_y^{12}-\frac{\tau_1^1}{2}+\pi_y^{12}+\tau_2^1\right), \tag{2.16}$$

with $\omega_0=\omega_1$ and delays

$$\tau_1^1=-\Omega T\left(\frac{1}{\pi J}+\frac{2}{(\omega_2-\omega_1)}\right), \tag{2.17}$$

$$\tau_2^1 = +2\Omega T\left(\frac{1}{(\omega_2-\omega_1)}\right).$$

The map ϕ_1 is related to ϕ_0 through the permutation $(ab)(cd)$. Other related mappings may be obtained from permutation considerations. These maps and others determine the subset of the control algebra over the physical system V_T, which will implement the desired unitary transformation U in the simulated system.

III. QUANTUM SIMULATION WITH RELAXATION

The effect of relaxation in the physical system on the result as it appears in the simulated system can be straightforwardly calculated once the implementation V_T is determined. This assumes that the relaxation is completely characterized. Since natural relaxation is tied to the physical system, two otherwise equivalent simulation mappings can yield different results. Furthermore, by combining such simulation steps or blocks [as described by the commutative diagram (2.1)] with different basis mappings, and exploiting certain symmetries, the final evolution of the simulated system may be modified to appear as if it occurred under a different effective relaxation. In the same way that quantum simulation without decoherence is an adaptation of AHT, the scheme described here is an adaptation of average Liouvillian theory [24,25].

The goal is to simulate an evolution of a reduced density matrix ρ_S under a Hamiltonian $\mathcal{H}_S$ and a relaxation superoperator Γ_S,

$$\rho_S(0) \xrightarrow{\mathcal{H}_S,\Gamma_S} \rho_S(T_f). \tag{3.1}$$

This may be implemented in several steps, where each step is a simulation implemented using a particular mapping,

$$\rho_S(0) \xrightarrow{\mathcal{H}_S} \rho_S(T) = \rho_S(T) \xrightarrow{\mathcal{H}_S} \rho_S(T+T') = \cdots. \tag{3.2}$$

The general scheme for simulation with decoherence using a physical system is given by the diagram (where the simulated time flows from left to right)

$$\begin{array}{ccccccccc}
\rho_S(0) & \xrightarrow{\mathcal{H}_S} & \rho_S(T) & = & \rho_S(T) & \xrightarrow{\mathcal{H}_S} & \rho_S(T+T') & = & \cdots \\
\phi_0\downarrow & & \uparrow\phi_0^{-1} & & \phi_1\downarrow & & \uparrow\phi_1^{-1} & & \\
\rho_P(0) & \xrightarrow{\mathcal{H}_P^0,\Gamma_P^0} & \rho_P(t_-) & \xrightarrow{U_{01}=(\phi_1\phi_0^{-1})} & \rho_P(t_+) & \xrightarrow{\mathcal{H}_P^1,\Gamma_P^1} & \rho_P(t+t') & \xrightarrow{U_{12}=(\phi_2\phi_1^{-1})} & \cdots.
\end{array} \tag{3.3}$$

The density operator ρ_S will evolve under $\mathcal{H}_S$ and Γ_S determined by Γ_P and the mappings ϕ_i. For example, $\Gamma_S = \Sigma_i \phi_i \Gamma_P \phi_i^{-1}$ for equal time blocks. Note that the simulation is faithful only at the beginning and end of each block, and that the transformation $U_{ij} = \phi_j \phi_i^{-1}$ is required in order to match the output of one simulation block to the appropriate input state of the next: $\rho_P(t_-) \to U_{ij} \to \rho_P(t_+)$. Each block is a simulation as described in the preceding section, but now generalized to include the effect of decoherence. In the implementation of V_T, the free evolutions will be governed by a relaxation matrix Γ_P, while we assume that the pulses in V_{T_i} are fast enough so that no relaxation takes place during them. The control available is limited by a time scale which is the time to implement each pulse sequence. Since the quantum simulation scheme presented here incorporates decoherence effects via a relaxation superoperator, it is a less restricted case than fast control processes which assume access to fast time scales. Furthermore, because of the controlled correspondence between physical and simulated times, long simulated time behavior may be explored.

Of particular interest here are those sequences of ϕ_i where $U_{ij} = \phi_i \phi_j^{-1}$ is a permutation that reflects a physical symmetry. For example, the unitary maps ϕ_i among the eigenstates in the two-spin case are just the $4! = 24$ permutation operations which are related to the logic gates for two spins as discussed by [38]. In NMR where there is a strongly quantizing field, the relaxation superoperator is simplified—in this case dominated by four parameters (see Appendix A). The maps we consider, ϕ_0 and ϕ_1, yield effective Hamiltonians involving $\{\sigma_z^2, \sigma_z^1\sigma_z^2\}$, while other maps would yield effective Hamiltonians involving $\{\sigma_z^1, \sigma_z^2\}$ or $\{\sigma_z^1, \sigma_z^1\sigma_z^2\}$. Any map will involve one or the other of the combinations of σ's and may be classified accordingly. The same maps can also be considered for the unitary transformations used to alter the effective decoherence. For the two-spin case, there are four (plus conditional versions) transformations (corresponding to $U_{ij} = \phi_i \phi_j^{-1}$) that are natural to consider: (i) Swap spin $1 \leftrightarrow$ spin 2, (bc) ZQT; (ii) flip both spins $|\uparrow\rangle \leftrightarrow |\downarrow\rangle$ (ad) DQT, (cb) ZQT; (iii) flip spin $2\,|\uparrow\rangle \leftrightarrow |\downarrow\rangle$ (ab) 1QT, (cd) 1QT; (iv) flip spin $1\,|\uparrow\rangle \leftrightarrow |\downarrow\rangle$ (ac) 1QT, (bd) 1QT; where ZQT, 1QT, and DQT refer to the zero, single, and double quantum transitions discussed in Appendix A. Suppose spin 1 decoheres rapidly, whereas spin 2 does not decohere at all. Then any simulation under a map ϕ_i is equivalent to a simulation under a map ϕ_j provided that $U_{ij} = \phi_i \phi_j^{-1}$ flips only spin 2. Moreover, if by symmetry considerations a subspace that is invariant under its decoherence operators [39,40] is also preserved by a transformation, then mappings related by that transformation are equivalent (and noiseless) for simulation within that subspace. Map-

pings that are noninvariant are useful for constructing a simulation with a modified decoherence behavior.

More generally, one would like to be able to homogenize the relaxation superoperator such that all terms decay with the same rate, allowing; one to create decoherence behavior as a deviation from an overall attenuation. While homogenization is possible for matrices under permutations of basis states, it is not fully possible for a superoperator. For an arbitrary $N\times N$ matrix R with no assumed symmetry, the sum over all possible $(N!)$ permutations of the basis states will average the off-diagonal elements with each other, and will average the diagonal elements with each other. For the off-diagonal elements

$$R_{ij}=2(N-2)!\sum_{k\neq l} R_{kl} \tag{3.4}$$

and for the diagonal elements

$$R_{ii}=(N-1)!\sum_{k} R_{kk} \tag{3.5}$$

giving, after summing over all permutation mappings,

$$\langle R\rangle = G[\mathbf{1}+e(\mathbf{J}-\mathbf{1})] \tag{3.6}$$

where $\mathbf{J}$ is the $N\times N$ matrix with all 1's. G represents an overall attenuation factor, and e is the off-diagonal contribution. Permutation operations alone will not equilibrate the diagonal with the off-diagonal values. Mappings ϕ that take a basis element to a linear combination of basis elements are needed to mix the diagonal with the nondiagonal terms. For a relaxation superoperator, however, the permutations among the basis states of the quantum system will not average all the transitions described by elements of the superoperator, Γ. For example, no basis state permutation is able to take Γ_{ijkl} to Γ_{ijil} $(k\neq i)$. In the secular approximation the terms Γ_{iiii} (T_1), Γ_{iijj} (nuclear Overhauser effect), and Γ_{ijij} (T_2) are allowed, whereas the terms Γ_{iiij}, Γ_{iijk}, Γ_{ijik}, and Γ_{ijkl} are not allowed. This means that by basis-state permutations one may homogenize each of the above three types of relaxation only among themselves. In any case, a simulation carried out using Eq. (3.3) appears as if evolution occurred under $\mathcal{H}_S,\Gamma_S$, where Γ_S equals the averaged relaxation $\langle\Gamma_P\rangle$. In practice, a smaller number of permutations may be enough to simplify Γ_S.

In general, calculation of the complete evolution of ρ under $\mathcal{H}_P$ as implemented by $V_T(\phi_i)$ involves free evolution under the internal Hamiltonian $\mathcal{H}_0$, and external interactions such as radio-frequency (RF) pulses in NMR, in addition to relaxation which is characterized by a superoperator Γ. For no relaxation, the evolution of ρ should be equivalent to evolution under $\mathcal{H}_{\rm int}$ alone. The Liouville density operator can be expanded in terms of basis operators where the appropriate choice of basis will be determined by the dynamics [41]. In this way, the final density matrix after V_T may be calculated. The Redfield matrix, Γ, for the case of two spins is given in Appendix A, and an analytical solution for evolution under Γ is given in Appendix B.

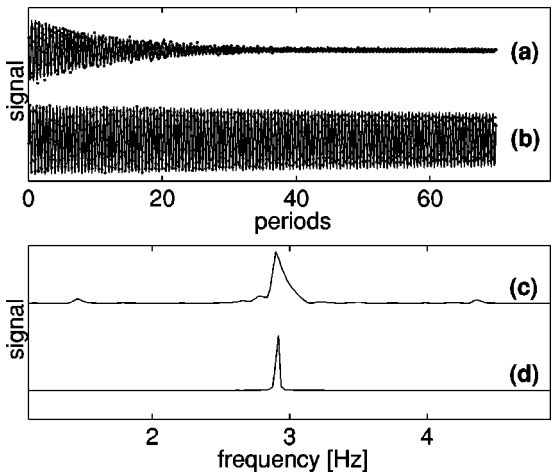

FIG. 2. NMR peak signals from 2,3-dibromothiophene demonstrating a quantum simulation of the $|0\rangle+i|2\rangle$ state of a truncated harmonic oscillator as implemented by the two mappings ϕ_0 and ϕ_1 displaying different effective relaxation: (a) the double quantum coherence state $|\uparrow\uparrow\rangle+|\downarrow\downarrow\rangle$ decays quickly (lifetime 4.7 sec, 13.6 periods) compared to (b) the zero quantum coherence state $|\uparrow\downarrow\rangle+|\downarrow\uparrow\rangle$ (lifetime 94 sec, 271 periods). 70 periods of simulated oscillation correspond to a physical time of 24.2 sec. The solid lines are exponentially damped sinusoids. The power spectra of (a) and (b) scaled to the same height are shown in (c) and (d). The linewidth of (d) is limited by the simulation sampling bandwidth; the spectra for longer simulations would be much sharper.

Simulation blocks using ϕ_0 or ϕ_1, for example, exhibit different relaxation behaviors in the simulated system due to the choice of mapping. In the general case where $\mathcal{H}_S\neq\mathcal{H}_{\rm int}$, the effect of relaxation must be worked out for each pulse sequence V_T. For the mappings ϕ_0 and ϕ_1, the pulse sequences V_T are particularly simple, and involve only π pulses and delays. A consequence of this is that the populations will be independent of the off-diagonal terms in the density matrix. The harmonic-oscillator state $|0\rangle+|2\rangle$, for example, when implemented using ϕ_0 and ϕ_1 on a two-spin homonuclear molecule, will correspond to $|\uparrow\downarrow\rangle+|\downarrow\uparrow\rangle(\phi_0)$ and $|\uparrow\uparrow\rangle+|\downarrow\downarrow\rangle(\phi_1)$. The state $|\uparrow\uparrow\rangle+|\downarrow\downarrow\rangle$ is known as a double quantum coherence (DQC) state, and will relax with a transverse magnetization relaxation rate $[(\sim T_2^{(a,b)})^{-1}]$. The state $|\uparrow\downarrow\rangle+|\downarrow\uparrow\rangle$ is known as a zero quantum coherence (ZQC) state, and will relax with a much slower rate $[(\sim T_2^{(c,d)})^{-1}]$. These relaxation rates contain an adiabatic contribution caused by independent fluctuations that change the energy-level difference. Multiple quantum relaxation rates such as $(\sim T_2^{(a,b)})^{-1}$ provide information not obtainable in general from single quantum relaxation measurements [41]. The experimental data verifying this behavior are shown in Fig. 2. The harmonic-oscillator state $|0\rangle+i|2\rangle$ when simulated under ϕ_1 corresponds to a double quantum coherence state which decays quickly compared to a simulation of the same harmonic-oscillator state under ϕ_0 corresponding to a zero quantum coherence state.

A pseudopure state $|\downarrow\downarrow\rangle$ [34] was prepared from a thermal equilibrium state using magnetic-field gradient techniques, and then converted to a superposition state corresponding to

the harmonic-oscillator state $|0\rangle+i|2\rangle$. Specifically, a pseudopure state was made using the following pulse sequence: $[\pi/4_x^{1,2}-1/4J-\pi_y^{1,2}-1/4J-\pi/6_y^{1,2}-G_y-\pi_y^1-G_x-G_y-\pi_x^2-G_x]$, where G refers to the application of a magnetic-field gradient along a given axis which with a spin-selective π pulse dephases the transverse magnetization including the zero quantum coherences. The pulse sequence $[\pi/2_y^{1,2}-1/4J-\pi_y^{1,2}-1/4J-\pi/2_y^{1,2}]$ then results in the initial superposition state $|0\rangle+i|2\rangle$. Other initial states were similarly prepared.

Next the pulse sequence V_T enforces the desired Hamiltonian $\overline{\mathcal{H}_P}$. The two proton spins of 2,3-dibromothiophene have a resonance frequency of 400 MHz in the 9.4 Tesla spectrometer (Bruker Instruments, AMX400) used here. The difference in frequencies of the two protons due to their chemical shifts is 227.2 Hz, with each resonance split by 5.7 Hz due to a scalar (J) coupling. The longitudinal magnetization relaxation time, measured using a standard inversion recovery sequence, is $T_1\sim 39$ s. The transverse magnetization relaxation time, measured using a standard Carr-Purcell-Meibloom-Gill sequence, is $T_2\sim 24$ s, while that using a Hahn echo sequence is $T_2\sim 16$ s. The experimental sequence V_T makes the system sensitive to long time scale behavior such as molecular diffusion through magnetic-field inhomogeneity. Since a correlated error decoherence model is relevant to our molecular sample, the double quantum relaxation is expected to be about a fourth of the Hahn echo T_2. This demonstrates that even within a given physical system, different pulse sequences can be sensitive to different decoherence processes.

IV. CONCLUSIONS

The flexibility in designing an effective decoherence behavior in the simulated system, perhaps in conjunction with some experimental control of the physical decoherence, suggests a broad method to approach the quantum simulation of open systems. First, it is possible to characterize completely how decoherence will effect a simulation. Second, appropriate choices of simulation mappings may take advantage of natural symmetries in order to modify by design the effective decoherence in the simulated system. Third, it should be possible to simplify decoherence effects in a simulation within certain subspaces. Future investigations may address the interplay of decoherence with ancilla degrees of freedom, or noiseless subspaces [39,40] for quantum simulation.

ACKNOWLEDGMENTS

We thank L. Viola for helpful discussions. This work was supported in part by the U.S. Army Research office under Contract/Grant No. DAAG 55-97-1-0342 from the DARPA Microsystems Technology Office. R.L. and E.K. acknowledge support by DOE under Contract No. W-7405-ENG-36. R.L. acknowledges support from the National Security Agency.

APPENDIX A: REDFIELD MATRIX

The matrix representation of the relaxation superoperator is called the Redfield matrix [41]. For the two-spin example, there are four energy eigenstates,

$$\begin{array}{ccc} & \underline{a\equiv|\uparrow\uparrow\rangle} & \\ \underline{b\equiv|\uparrow\downarrow\rangle} & & \underline{c\equiv|\downarrow\uparrow\rangle} \\ & \underline{d\equiv|\downarrow\downarrow\rangle} & \end{array} \tag{A1}$$

The 4×4 reduced density matrix is obtained after tracing over the environment variables: $\rho=\mathrm{tr}_R\rho_0$. The diagonal elements are the populations of the states, and the off-diagonal elements are the zero-, single-, or double-quantum transition operators. These 16 elements can be arranged in the Liouville space column vector,

$$\rho=\begin{pmatrix}\rho_{11}\\ \rho_{12}\\ \vdots\\ \rho_{44}\end{pmatrix}. \tag{A2}$$

Evolution is governed by the Liouville–von Neumann master equation:

$$\dot\rho(t)=-i[\mathcal{H}_0,\rho(t)]+\Gamma\{\rho(t)-\rho_{\mathrm{eq}}\}. \tag{A3}$$

The ρ_{eq} refers to the thermal equilibrium density matrix, which for two spin-$\frac{1}{2}$ particles with gyromagnetic ratios γ_I,γ_S is

$$\rho_{\mathrm{eq}}=\frac{1}{4}\mathbf{1}+(\hbar B/8kT)\mathrm{diag}[\gamma_I+\gamma_S,\gamma_I-\gamma_S,-\gamma_I+\gamma_S,-\gamma_I-\gamma_S], \tag{A4}$$

in the $\{|\uparrow\uparrow\rangle, |\uparrow\downarrow\rangle, |\downarrow\uparrow\rangle, |\downarrow\downarrow\rangle\}$ basis in the approximation of large T and small J coupling. The relaxation superoperator Γ maps density operators to density operators, and is in general not invertible. Superoperators effect a mapping among the algebra of operators that act in Liouville space, whereas operators effect a mapping among the state vectors in Hilbert space. In the interaction picture,

$$\dot\Delta\rho_P=-\Gamma_P\Delta\rho_P, \tag{A5}$$

where $\Delta\rho_P=\rho_P-\rho_{\mathrm{eq}}$. In the secular approximation, this is the block-diagonal ''Redfield kite'' matrix. For two spins, the 16×16 Redfield matrix, Γ, is

$$\mathbf{\Gamma}=\begin{bmatrix} W & 0 & 0 & 0\\ 0 & \Gamma_0 & 0 & 0\\ 0 & 0 & \Gamma_1 & 0\\ 0 & 0 & 0 & \Gamma_2\end{bmatrix}. \tag{A6}$$

This is composed of the following.

(i) A 4×4 block of transformations among the populations with $W_{ii}=-\Sigma_{i\neq j}W_{ij}$ and $W_{ij}=J_{ijij}(\omega_{ij})$, where J is the power spectral density and $\omega_{ii}=0$:

$$\{|\uparrow\uparrow\rangle\langle\uparrow\uparrow|,\ |\uparrow\downarrow\rangle\langle\uparrow\downarrow|,\ |\downarrow\uparrow\rangle\langle\downarrow\uparrow|,\ |\downarrow\downarrow\rangle\langle\uparrow\uparrow|\},$$

$$\mathbf{W}=\begin{bmatrix}\Gamma_a & \Gamma^I & \Gamma^S & \Gamma_{(2)}\\ \Gamma^I & \Gamma_b & \Gamma_{(0)} & \Gamma^S\\ \Gamma^S & \Gamma_{(0)} & \Gamma_b & \Gamma^I\\ \Gamma_{(2)} & \Gamma^S & \Gamma^I & \Gamma_a\end{bmatrix}; \tag{A7}$$

(ii) a 2×2 diagonal block of transformations among the zero-quantum transition operators with $\omega_{\alpha\alpha'}=J$ and with $\Gamma_0^1=\Gamma_0^2$:

$$\{|\uparrow\downarrow\rangle\langle\downarrow\uparrow|,\ |\downarrow\uparrow\rangle\langle\uparrow\downarrow|\},$$

$$\mathbf{\Gamma}_0=\begin{bmatrix}\Gamma_0^1 & 0\\ 0 & \Gamma_0^1\end{bmatrix}; \tag{A8}$$

(iii) an 8×8 diagonal block of transformations among the single-quantum transition operators:

$$\{|\uparrow\uparrow\rangle\langle\uparrow\downarrow|,\ |\uparrow\downarrow\rangle\langle\uparrow\uparrow|,\ |\uparrow\uparrow\rangle\langle\downarrow\uparrow|,\ |\downarrow\uparrow\rangle\langle\uparrow\uparrow|,$$
$$|\uparrow\downarrow\rangle\langle\downarrow\downarrow|,\ |\downarrow\downarrow\rangle\langle\uparrow\downarrow|,\ |\downarrow\uparrow\rangle\langle\downarrow\downarrow|,\ |\downarrow\downarrow\rangle\langle\downarrow\uparrow|\}$$

with $\omega_{\alpha\alpha'}=(\omega_I-\omega_0)\pm J/2$ and with $\Gamma_1^{ab}=\Gamma_1^{cd},\Gamma_1^{ac}=\Gamma_1^{bd}$:

$$\mathbf{\Gamma}_1=\mathrm{diag}[\Gamma_1^1,\ \Gamma_1^1,\ \Gamma_1^3,\ \Gamma_1^3,\ \Gamma_1^3,\ \Gamma_1^3,\ \Gamma_1^1,\ \Gamma_1^1]; \tag{A9}$$

(iv) a 2×2 diagonal block of transformations among the double-quantum transition operators:

$$\{||\uparrow\uparrow\rangle\langle\uparrow\uparrow|,\ |\downarrow\downarrow\rangle\langle\uparrow\uparrow|\}$$

with $\omega_{\alpha\alpha'}=\omega_1+\omega_2$ with $\Gamma_2^1=\Gamma_2^2$:

$$\mathbf{\Gamma}_2=\begin{bmatrix}\Gamma_2^1 & 0\\ 0 & \Gamma_2^2\end{bmatrix}. \tag{A10}$$

The correlation time of the bath should be much shorter than the evolution time or the longitudinal or transverse relaxation times. For $\alpha=\alpha'$, $\rho_{\alpha\alpha'}(t)=\Sigma_i A_{\alpha i}e^{-\lambda_i t}$, where λ_i are eigenvalues of $W(\rho_{\alpha\alpha'}(\infty)=\rho_{\alpha\alpha'\mathrm{eq}})$. For $\alpha\neq\alpha'$, $\rho_{\alpha\alpha'}=\rho_{\alpha\alpha'}(0)e^{i\omega_{\alpha\alpha'}t}e^{-\Gamma_{\alpha\alpha'}t}$. In the two-spin case, the populations will relax according to the Solomon equations (see Appendix B).

APPENDIX B: SOLUTION TO THE SOLOMON EQUATIONS

The populations are governed by

$$\Delta\rho_{\alpha\alpha}(t)=e^{-Wt}\Delta\rho_{\alpha\alpha}(0). \tag{B1}$$

The population matrix W is block diagonal in the Cartesian basis. The matrix $\mathbf{Q}$ transforms the Cartesian basis $\{\frac{1}{2}\mathbf{1},S_z,I_z,2I_zS_z\}$ to the binary ordered Zeeman basis $\{|a\rangle\times\langle a|,|b\rangle\langle b|,|c\rangle\langle c|,|d\rangle\langle d|\}$.

$$\mathbf{Q}=\frac{1}{2}\begin{bmatrix}1 & 1 & 1 & 1\\ 1 & -1 & 1 & -1\\ 1 & 1 & -1 & -1\\ 1 & -1 & -1 & 1\end{bmatrix}, \tag{B2}$$

where it is easy to verify that

$$\mathbf{Q}^{-1}=\mathbf{Q}.$$

This is just the $2^2\times2^2$ Hadamard matrix [37]. In the Cartesian basis, the population block of the Redfield matrix is then

$$-\mathbf{Q}^{-1}\mathbf{W}\mathbf{Q}=\begin{bmatrix}0 & 0 & 0 & 0\\ 0 & -2\Gamma^S-(\Gamma_{(0)}+\Gamma_{(2)}) & (\Gamma_{(0)}-\Gamma_{(2)}) & 0\\ 0 & (\Gamma_{(0)}-\Gamma_{(2)}) & -2\Gamma^I-(\Gamma_{(0)}+\Gamma_{(2)}) & 0\\ 0 & 0 & 0 & -2(\Gamma^I+\Gamma^S)\end{bmatrix}, \tag{B3}$$

where each matrix element is negative, and $\Gamma^{S,I},\Gamma_{(0,2)}>0$. The upper left element is zero indicating that the **1** component does not decay. The middle 2×2 block is the Solomon matrix $\mathcal{R}$. The evolution of the populations may be solved in closed form as follows. Define the autorelaxation elements

$$\rho_S=-2\Gamma^S-(\Gamma_{(0)}+\Gamma_{(2)}),$$
$$\rho_I=-2\Gamma^I-(\Gamma_{(0)}+\gamma_{(2)}), \tag{B4}$$

and the cross-relaxation elements

$$\rho_{IS}=(\Gamma_{(0)}-\Gamma_{(2)}). \tag{B5}$$

The exponential of the relaxation matrix is [42]

$$\exp(tQ^{-1}WQ)=\begin{bmatrix} 1 & 0 & 0 & 0 \\ 0 & e^{t\alpha}[\cosh(t\beta)+\delta\sinh(t\beta)/\beta] & e^{t\alpha}[\rho_{IS}\sinh(t\beta)/\beta] & 0 \\ 0 & e^{t\alpha}[\rho_{IS}\sinh(t\beta)/\beta] & e^{t\alpha}[\cosh(t\beta)-\delta\sinh(t\beta)/\beta] & 0 \\ 0 & 0 & 0 & e^{-2(\Gamma^I+\Gamma^S)t} \end{bmatrix}$$

$$\equiv\begin{bmatrix} 1 & 0 & 0 & 0 \\ 0 & e^{t\alpha}A^+ & e^{t\alpha}B & 0 \\ 0 & e^{t\alpha}B & e^{t\alpha}A^- & 0 \\ 0 & 0 & 0 & C \end{bmatrix}, \tag{B6}$$

where

$$\begin{aligned} \alpha&=(\rho_S+\rho_I)/2, \\ \beta^2&=\delta^2+\rho_{IS}^2, \\ \delta&=(\rho_S-\rho_I)/2, \end{aligned} \tag{B7}$$

and the parameters A,B depend on time. The relaxation of the deviation of the traceless part of the populations from equilibrium after a time t is given by

$$\Delta\rho_P(0)=\begin{bmatrix} p_{aa} \\ p_{bb} \\ p_{cc} \\ p_{dd} \end{bmatrix} \xrightarrow{Q^{-1}} \begin{bmatrix} (p_{aa}+p_{bb}+p_{cc}+p_{dd} \\ \frac{1}{2}(p_{aa}-p_{bb}+p_{cc}-p_{dd}) \\ \frac{1}{2}(p_{aa}+p_{bb}-p_{cc}-p_{dd}) \\ \frac{1}{2}(p_{aa}-p_{bb}-p_{cc}+p_{dd}) \end{bmatrix}$$

$$\xrightarrow{e^{tQ^{-1}WQ}} \begin{bmatrix} 1 \\ \frac{1}{2}[(p_{aa}-p_{bb}+p_{cc}-p_{dd})A^+ +(p_{aa}+p_{bb}-p_{cc}-p_{dd})B]e^{t\alpha} \\ \frac{1}{2}[(p_{aa}-p_{bb}+p_{cc}-p_{dd})B+(p_{aa}+p_{bb}-p_{cc}-p_{dd})A^-]e^{t\alpha} \\ \frac{1}{2}(p_{aa}-p_{bb}-p_{cc}+p_{dd})C \end{bmatrix}$$

$$\xrightarrow{Q} \frac{1}{4}\begin{bmatrix} (1+e^{t\alpha}[(p_{aa}-p_{bb}+p_{cc}-p_{dd})(+A^++B)+(p_{aa}+p_{bb}-p_{cc}-p_{dd})(+A^-+B)]+(p_{aa}-p_{bb}-p_{cc}+p_{dd})C]) \\ (1+e^{t\alpha}[(p_{aa}-p_{bb}+p_{cc}-p_{dd})(-A^++B)+(p_{aa}+p_{bb}-p_{cc}-p_{dd})(+A^--B)]-(p_{aa}-p_{bb}-p_{cc}+p_{dd})C]) \\ (1+e^{t\alpha}[(p_{aa}-p_{bb}+p_{cc}-p_{dd})(+A^+-B)+(p_{aa}+p_{bb}-p_{cc}-p_{dd})(-A^-+B)]-(p_{aa}-p_{bb}-p_{cc}+p_{dd})C]) \\ (1+e^{t\alpha}[(p_{aa}-p_{bb}+p_{cc}-p_{dd})(-A^+-B)+(p_{aa}+p_{bb}-p_{cc}-p_{dd})(-A^--B)]+(p_{aa}-p_{bb}-p_{cc}+p_{dd})C]) \end{bmatrix}. \tag{B8}$$

[1] D. F. Walls and G. J. Milburn, *Quantum Optics* (Springer-Verlag, Berlin/Heidelberg, 1995).
[2] W. P. Schleich, Nature (London) **403**, 256 (2000).
[3] C. J. Myatt, B. E. King, Q. A. Turchette, C. A. Sackett, D. Kielpinski, W. M. Itano, C. Monroe, and D. J. Wineland, Nature (London) **403**, 269 (2000).
[4] R. P. Feynman, Found. Phys. **16**, 507 (1986).
[5] S. Lloyd, Science **263**, 1569 (1993).
[6] C. H. Bennett, Phys. Today **48** (10), 24 (1995).
[7] D. Divincenzo, Science **270**, 255 (1995).
[8] P. W. Shor, Phys. Rev. A **52**, R2493 (1995).
[9] A. M. Steane, Phys. Rev. Lett. **77**, 793 (1996).
[10] R. Laflamme, C. Miquel, J. P. Paz, and W. H. Zurek, Phys. Rev. Lett. **77**, 198 (1996).
[11] A. Ekert and C. Macchiavello, Phys. Rev. Lett. **77**, 2585 (1996).
[12] C. H. Bennett, D. P. DiVincenzo, J. A. Smolin, and W. K. Wootters, Phys. Rev. A **54**, 3824 (1996).
[13] D. Divincenzo and P. W. Shor, Phys. Rev. Lett. **77**, 3260 (1996).
[14] E. Knill and R. Laflamme, Phys. Rev. A **55**, 900 (1997).
[15] E. Knill, R. Laflamme, and W. H. Zurek, Science **279**, 342 (1998).
[16] D. G. Cory, M. D. Price, W. Maas, E. Knill, R. Laflamme, W. H. Zurek, T. F. Havel, and S. S. Somaroo, Phys. Rev. Lett. **81**, 2152 (1998).
[17] W. S. Warren, H. Rabitz, and M. Dahleh, Science **259**, 1581 (1993).

[18] R. J. Nelson, D. G. Cory, and S. Lloyd, Phys. Rev. A **61**, 022106 (2000).
[19] M. Ban, J. Mod. Opt. **45**, 2315 (1998).
[20] L. Viola, E. Knill, and S. Lloyd, Phys. Rev. Lett. **82**, 2417 (1999).
[21] L. Viola, E. Knill, and S. Lloyd, Phys. Rev. Lett. **83**, 4888 (1999).
[22] J. P. Barnes and W. S. Warren, Phys. Rev. A **60**, 4363 (1999).
[23] S. Somaroo, C. H. Tseng, T. F. Havel, R. Laflamme, and D. G. Cory, Phys. Rev. Lett. **82**, 5381 (1999).
[24] M. H. Levitt and L. G. D. Bari, Phys. Rev. Lett. **69**, 3124 (1992).
[25] R. Ghose, T. R. Eykyn, and G. Bodenhausen, Mol. Phys. **96**, 1281 (1999).
[26] R. P. Feynman, Int. J. Theor. Phys. **21**, 467 (1982).
[27] S. Lloyd, Science **273**, 1073 (1996).
[28] C. Zalka, Proc. R. Soc. London **454**, 313 (1998).
[29] D. S. Abrams and S. Lloyd, Phys. Rev. Lett. **79**, 2586 (1997).
[30] D. A. Lidar and O. Biham, Phys. Rev. E **56**, 3661 (1997).
[31] A. Barenco, B. C. H, R. C. , D. P. DiVincenzo, N. Margolus, P. Shor, T. Sleator, J. A. Smolin, and H. Weinfurter, Phys. Rev. A **52**, 3457 (1995).
[32] S. Lloyd, Phys. Rev. Lett. **75**, 346 (1995).
[33] J. S. Waugh, *Encyclopedia Of NMR* (Wiley, New York, 1996), Vol. 2, pp. 849–854.
[34] D. Cory, A. Fahmy, and T. Havel, Proc. Natl. Acad. Sci. USA **94**, 1634 (1997).
[35] N. A. Gershenfeld and I. L. Chuang, Science **275**, 350 (1997).
[36] C. H. Tseng, S. Somaroo, Y. Sharf, E. Knill, R. Laflamme, T. F. Havel, and D. G. Cory, Phys. Rev. A **61**, 012 302 (2000).
[37] V. Maz'ya and T. Shaposhnikova, *Jacques Hadamard, A Universal Mathematician* (American Mathematical Society and London Mathematical Society, Hartford, 1998).
[38] M. D. Price, S. S. Somaroo, C. H. Tseng, J. C. Gore, A. F. Fahmy, T. F. Havel, and D. G. Cory, J. Magn. Reson., Ser. A **140**, 371 (1999).
[39] P. Zanardi and M. Rasetti, Phys. Rev. Lett. **79**, 3306 (1997).
[40] D. A. Lidar, I. L. Chuang, and K. B. Whaley, Phys. Rev. Lett. **81**, 2594 (1998).
[41] R. Ernst, G. Bodenhausen, and A. Wokaun, *Principles Of NMR In One And Two Dimensions* (Clarendon Press, Oxford, 1987).
[42] I. Najfield, K. T. Dayie, G. Wagner, and T. F. Havel, J. Magn. Reson., Ser. A **124**, 372 (1997).